EUROPEAN SYNCHROTRON RADIATION FACILITY

INSTALLATION EUROPEENNE DE RAYONNEMENT SYNCHROTRON

ESRF

Experiment Report Form

The double page inside this form is to be filled in by all users or groups of users who have had access to beam time for measurements at the ESRF.

Once completed, the report should be submitted electronically to the User Office via the User Portal:

https://wwws.esrf.fr/misapps/SMISWebClient/protected/welcome.do

Reports supporting requests for additional beam time

Reports can be submitted independently of new proposals – it is necessary simply to indicate the number of the report(s) supporting a new proposal on the proposal form.

The Review Committees reserve the right to reject new proposals from groups who have not reported on the use of beam time allocated previously.

Reports on experiments relating to long term projects

Proposers awarded beam time for a long term project are required to submit an interim report at the end of each year, irrespective of the number of shifts of beam time they have used.

Published papers

All users must give proper credit to ESRF staff members and proper mention to ESRF facilities which were essential for the results described in any ensuing publication. Further, they are obliged to send to the Joint ESRF/ ILL library the complete reference and the abstract of all papers appearing in print, and resulting from the use of the ESRF.

Should you wish to make more general comments on the experiment, please note them on the User Evaluation Form, and send both the Report and the Evaluation Form to the User Office.

Deadlines for submission of Experimental Reports

- 1st March for experiments carried out up until June of the previous year;
- 1st September for experiments carried out up until January of the same year.

Instructions for preparing your Report

- fill in a separate form for each project or series of measurements.
- type your report, in English.
- include the reference number of the proposal to which the report refers.
- make sure that the text, tables and figures fit into the space available.
- if your work is published or is in press, you may prefer to paste in the abstract, and add full reference details. If the abstract is in a language other than English, please include an English translation.

ESRF	**Experiment title:** Probing the magnetic coupling of Nickel and Cobalt embedded in a 2D metal-organic framework on Au(111) via XMCD.	**Experiment number**: MA-3668
Beamline: ID 32	**Date of experiment**: from: 21/02/2018 to: 27/02/2018	**Date of report**: 14/05/2018
Shifts: 3 per day	**Local contact(s)**: Davide Betto (davide.betto@esrf.fr).	*Received at ESRF:*

Names and affiliations of applicants (* indicates experimentalists):

Prof. Dr. Meike Stöhr – University of Groningen.

Dr. Mihaela Enache – University of Groningen.

Nico Schmidt – University of Groningen.

Brian David Baker – University of Groningen.

Report:

The study of the self-assembly of two-dimensional (2D) metal-organic coordination networks (MOCNs) exhibiting magnetic coupling has increased in the past few years [1]. The usage of versatile molecular building blocks with magnetic metallic centers, such as porphyrin derivatives allow the formation of periodic 2D arrays displaying magnetic coupling given by the unpaired d-electrons of transition metals contained within the porhpyrin core. The magnetic properties of these networks can be investigated by means of X-ray magnetic circular dichroism (XMCD) [2-3]. The aim of our XMCD measurements was to investigate the magnetic coupling of the two transition metals Nickel (embedded in the porphyrin core) and Cobalt (acting as coordinating metal center) embedded in a 2D MOCN adsorbed on a non-magnetic surface.

Before coming to the ID32 beamline, we investigated the self-assembly of periodic 2D networks formed by Co and Ni porphyrin derivatives supported on Au(111) and graphene/Ir(111) with scanning tunneling microscopy (STM) and low-energy electron diffraction (LEED) at our home laboratory at the Zernike Institute for Advanced Materials at University of Groningen. The molecules were deposited onto the substrates by thermal evaporation, while keeping the substrates at RT. All experiments were carried under ultrahigh vacuum (UHV) conditions. We employed 4 different types of porphyrin derivatives: Nickel(II) 5,10, 15, 20-(tetra-4-cyanophenyl)porphyrin (Ni-TCPP), Cobalt(II) 5,10, 15, 20-(tetra-4-cyanophenyl)porphyrin (Co-TCPP), Nickel (II) (5,15-dipentyl-10,20-(4-yl-pyridine)porphyrin (Ni-DPPyP) and Nickel (II) (5,15-dihexyl-10,20-(4-yl-pyridine)porphyrin (Ni-DHPyP).

For the cyanophenyl porphyrin derivatives (Ni-TCPP and Co-TCPP) we report the formation of a close-packed H-bonded network on either Au(111) or grahpene/Ir(111). Upon deposition of Co-atoms onto the networks supported on Au(111), a 4-fold Co-coordination takes place, where one Co-atom coordinates to 4 cyano substituents of neighboring cyanophenyl porphyrins. Similarly, both Ni-DPPyP and Ni-DHPyP compounds form a H-bonded network on Au(111). The deposition of cobalt atoms onto both of these close-packed networks and subsequent annealing at 150 ℃ lead to the formation of a Co-coordinated hexagonal porous network. We aimed to reproduce our 2D molecular networks at the ID32 beamline. The Au(111) and Ir(111) crystals were cleanned by repeated cycles of sputtering with Ar^+ ions and annealing. Graphene was

grown on Ir(111) at the electron beam heating stage by using ethylene as carbon precursor and mainting the substrate at 1,100 °C. The molecules were thermally evaporated from our evaporator and the deposition rate was monitored via a quartz crystal microbalance. The molecule evaporator and quartz microbalance were mounted to a 6-way cross adapted to the load lock chamber. Co-atoms were deposited from a rod using an e-beam metal evaporator provided by the beamline ID32. The 2D networks were analyzed at RT with an Omicron VT-STM to corroborate their structural arrangement with our previous findings. We were not able to reproduce the systems for Ni-DPPyP and Ni-DHPyP due to evaporation problems and therefore proceeded to only measure the cyanophenyl derivatives.

We performed XMCD measurements at the ID32 beamline under different conditions. Measurements of the Co and Ni $L_{2;3}$ edges for the 2D networks were done at normal and grazing incidence, the magnetic field (B) was varied between 9 T and -9 T for various measurements. The acquired spectra were analyzed with the PyMca software. This software provided a fast analysis to obtain the XMCD signal by obtaining the difference ($\mu^- - \mu^+$) between left and right circularly polarized spectra. Aditionally, the magnetization curves for samples of Co-TCPP on Au(111) and on graphene/Ir(111) were obtained.

The XMCD spectra shown in Fig. 1 were obtained at normal incidence ($\theta = 0°$) with a mangetic field of 9 T. The top row corresponds to the X-ray absorption (XAS) measurements of the Co $L_{2;3}$ absorption edge for (a) Co-TCPP on Au(111), (b) Co-TCPP on Au(111) with Co-atoms and (c) bare Co-atoms on Au(111). The scans obtained with left and right circularly polarized light are denoted by the blue and red lines, respectively. The bottom row of Fig. 1 contains the XMCD signal for each of the aforementioned 2D networks (a-d, b-e and c-f, respectively). The Co L_3 and L_2 edges are clearly visible in the XAS spectra (top row). The dichroic signal is only present in the spectra shown in (e) and (f).
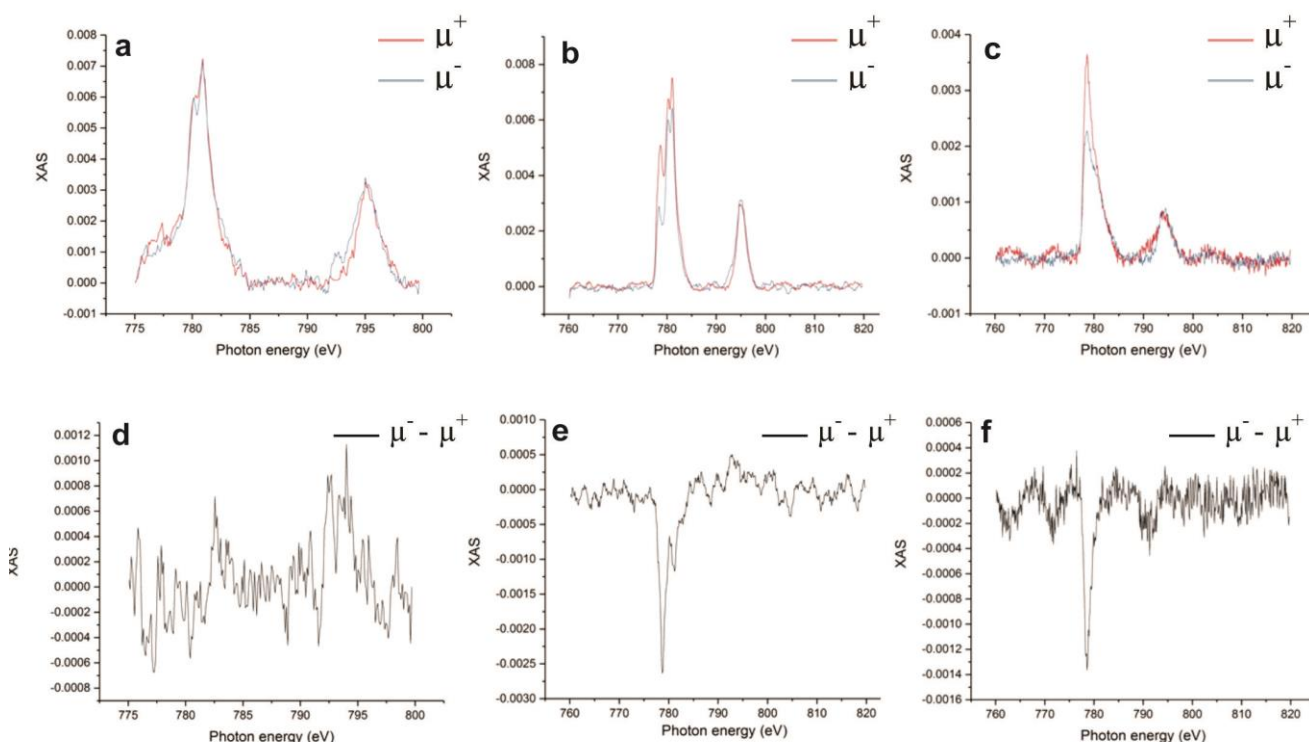

Figure 1. XMCD spectra for 3 different types of 2D networks supported on Au(111): (a-d) Co-TCPP H-bonded network, (b-e) Co-TCPP 4-fold Co-coordinated network and (c-f) bare Co-atoms. Top row: XAS taken with left and right circularly polarized X-rays. Bottom row: XMCD signal taken by the difference ($\mu^- - \mu^+$) between left (μ^-) and right (μ^+) circularly polarized X-rays.

The XMCD spectra in Fig. 2 taken at normal incidence ($\theta = 0°$) with a mangetic field of 9 T belong to 2D networks supported on graphene/Ir(111). The top row displays the X-ray absorption (XAS) measurements of the Co $L_{2;3}$ absorption edge for (a) Co-TCPP and the Ni $L_{2;3}$ absorption edge for (b) Ni-TCPP and (c) multilayer coverage of Ni-TCPP. The multilayer Ni-TCPP network shown in Fig. 2(c-f) was prepared to compare the influence of additional molecular layers with respect so monolayer coverages, as depicted in Fig.

2(b-e) The scans obtained for left and right circularly polarized light are marked in blue and red, respectively. Following the same structure of Fig. 1, the XMCD signals shown in the bottom row of Fig.2 correspond to the XAS spectra of (a), (b) and (c). The dichroic signal is only present in the spectra shown in (d) and (f). Further analysis of the XAS peaks of our 2D networks is required to identify the underlying reason.
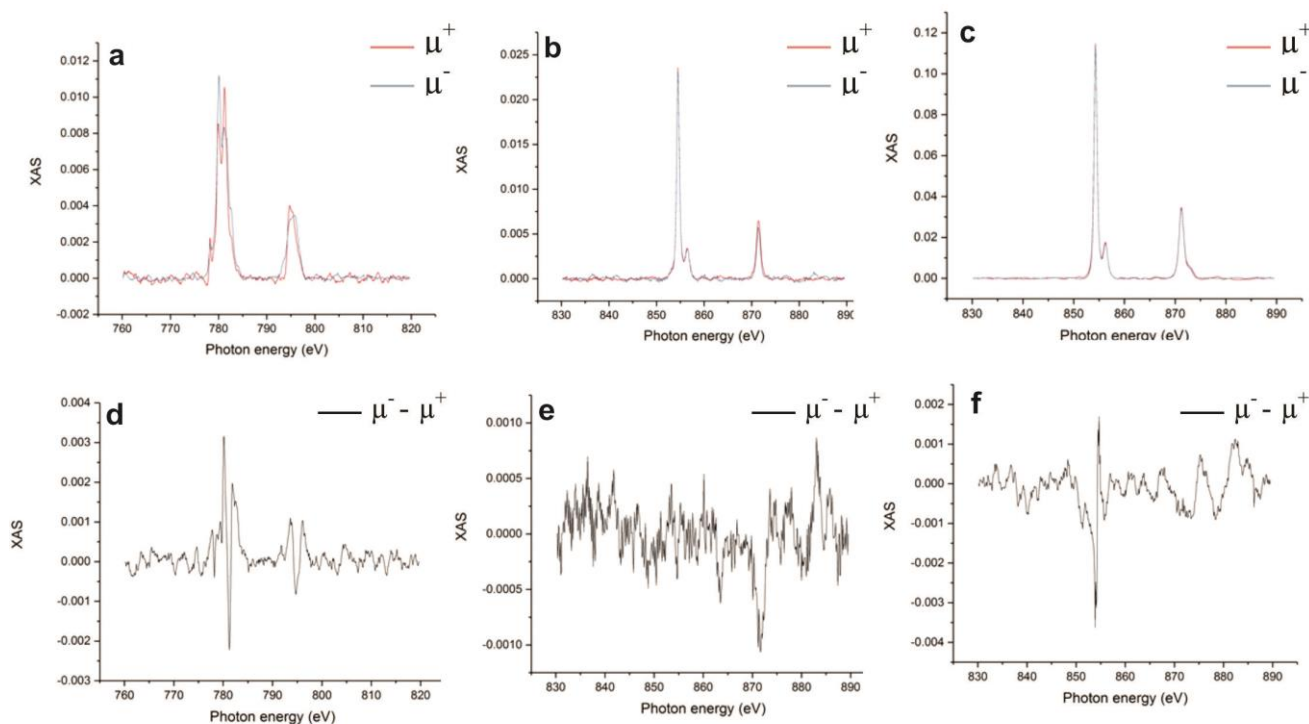

Figure 2. XMCD spectra for 3 different types of H-bonded 2D networks supported on graphene/Ir(111): (a-d) Co-TCPP H-bonded network, (b-e) Ni-TCPP H-bonded network and (c-f) multilayer of Ni-TCPP H-bonded network. Top row: XAS taken with left and right circularly polarized X-rays. Bottom row: XMCD signal taken by the difference (μ^- - μ^+) between left (μ^-) and right (μ^+) circularly polarized X-rays.

References.
[1] W. Kuch et al., J. Phys. Condens. Matter. 29 (2017) 023001.
[2] S. Vijayaraghavan et al., ACS Nano. 9 (2015) 507346.
[3] G. Avvisati et al., Nano Lett. 18 (2018) 04836.